Edge states in the integer quantum Hall effect and the Riemann surface of the Bloch function

Yasuhiro Hatsugai*
Institute for Theoretical Physics, University of California, Santa Barbara, California 93106
and Institute for Solid State Physics, University of Tokyo, 7-22-1 Roppongi, Minato-ku, Tokyo 106, Japan
(Received 27 May 1992; revised manuscript received 1 April 1993)

We study edge states in the integral quantum Hall effect on a square lattice in a rational magnetic field $\phi = p/q$. The system is periodic in the y direction but has two edges in the x direction. We have found that the energies of the edge states are given by the zero points of the Bloch function on some Riemann surface (RS) (complex energy surface) when the system size is commensurate with the flux. The genus of the RS, $g = q - 1$, is the number of the energy gaps. The energies of the edge states move around the holes of the RS as a function of the momentum in the y direction. The Hall conductance σ_{xy} is given by the winding number of the edge states around the holes, which gives the Thouless, Kohmoto, Nightingale, and den Nijs integers in the infinite system. This is a topological number on the RS. We can check that σ_{xy} given by this treatment is the same as that given by the Diophantine equation numerically. Effects of a random potential are also discussed.

I. INTRODUCTION

A problem of electrons in a magnetic field is an old problem and studied extensively in relation to the quantum Hall effect.[1–11] Even if the electron-electron interaction is absent, this problem is highly nontrivial when we consider the system of lattices.[5,12–17] In this case, there is no ambiguity such as the Peierls substitution. It provides many fundamental results including both effects of the periodic potential and the magnetic field accurately. This problem was also focused in the study of the high-temperature superconductivity. Some mean-field Hamiltonians of the high-temperature superconductivity are given by those of the lattice fermions.[18–24,17,25] Recently there have also been some studies for the three-dimensional quantum Hall effect and related topics.[25–29]

The Hall conductance of the system has a fundamental meaning which was first found by Thouless, Kohmoto, Nightingale and den Nijs (TKNN).[5] A tight-binding Hamiltonian of electrons on a square lattice under a uniform magnetic field is given by

$$H = -t_x \sum_{m,n} c^\dagger_{m+1,n} e^{i\theta_{m+1,n;m,n}} c_{m,n} -t_y \sum_{m,n} c^\dagger_{m,n+1} e^{i\theta_{m,n+1;m,n}} c_{m,n} + \text{H.c.} , \qquad (1.1)$$

where $c_{m,n}$ is an annihilation operator of a lattice fermion at a site (m,n) and $\sum_{\text{plaquett}} \theta_{\vec{r}} = 2\pi\phi$. In this paper, we assume the magnetic field is rational $\phi = p/q$ with mutually prime integers p and q. When the boundary condition is periodic or the system size is infinite, the problem is well investigated and the Hall conductance is quantized as some integral values when the Fermi energy lies in the energy gap.[5,9] This is the famous TKNN integer and it is a topological invariant (the first Chern number) on the magnetic Brillouin zone which is a torus.[8,16,30–32]

The free boundary condition was treated on the lattice by Rammal, Toulouse, Jaekel, and Halperin.[33] They performed numerical studies and concluded that the number of the edges states is related to the Hall conductance of the system even if there exists a periodic potential. This is an extension of Halperin's treatment of the edge states without the periodic potential.[4] There are also some numerical studies for the edge states.[34–37]

In this paper, we treat the problem analytically using techniques in the one-dimensional nonlinear lattice. Further we performed extensive numerical studies based on the analytical results. We found that there is a fundamental relation between the Hall conductance σ_{xy} and a *new topological number on a Riemann surface.* This topological number is different from the first Chern number of the TKNN by definition. This means we relate the TKNN integer to the other topological number. It is also known that the TKNN integers are given by the Diophantine equation.[5,10,17,38] Here we can confirm that our topological numbers coincide to those of the Diophantine equation for rational flux $\phi = p/q$ cases with rather small q ($\lesssim 13$). Some analytical arguments are also included.

In Sec. II we reduce the problem in two dimensions to that in one dimension to use a nonlinear lattice theory in one dimension. In Sec. III we discuss energy bands (bulk states) and edge states in detail. Some parts of Secs. II and III are a review of the previous works[5,14,15] and new results are their relation to the edge states. In Sec. IV we prove that the energies of the edges states give zero points of the Bloch function on the Riemann surface (complex energy surface) where the genus of the surface is the number of the energy gap. We perform detailed investigations about the Laughlin-Halperin argument[2,4] on this lattice system. We find the Hall conductance is given by the winding number of the energy of the edge state on the Riemann surface. This winding number is given by the intersection number of two curves on the Riemann surface. In this section, we treat a commensurate case.

0163-1829/93/48(16)/11851(12)/$06.00

In Sec. V we treat an incommensurate system and also discuss the randomness. Section VI is a summary of the work.

II. REDUCTION TO A ONE-DIMENSIONAL PROBLEM

In the Hamiltonian Eq. (1.1), we take a Landau gauge, that is, $\theta_{m+1,n;m,n} = 0$ and $\theta_{m,n+1;m,n} = 2\pi\phi m$. The Hamiltonian in this gauge is given by

$$H = -t_x \sum_{m,n} c^\dagger_{m+1,n} c_{m,n} - t_y e^{i\frac{2\pi\Phi}{L_y}} \sum_{m,n} c^\dagger_{m,n+1} e^{i2\pi\phi m} c_{m,n} + \text{H.c.}, \qquad (2.1)$$

where we assume that the system size is L_y in the y direction and impose a periodic boundary condition in the y direction. The factor $e^{i\frac{2\pi\Phi}{L_y}}$ represents flux Φ (in a unit of flux quantum $\Phi_0 = hc/e$) through the hole (Fig. 1). We assume that the system is finite for the x direction. This is the Laughlin-Halperin geometry[2,4] (Fig. 1). There are two edges and the number of sites is $L_x - 1$ in the x direction.

We use a momentum representation in the y direction

$$c_{m,n} = \frac{1}{\sqrt{L_y}} \sum_{k_y} e^{ik_y n} c_m(k_y), \qquad (2.2)$$

where k_y takes discrete value $k_y = 2\pi\frac{n_y}{L_y}$, $n_y = 1, \ldots, L_y$. Let us consider a one-particle state $|\Psi(k_y,\Phi)\rangle = \sum_m \Psi_m(k_y,\Phi) c^\dagger_m(k_y)|0\rangle$. Inserting it into the Schrödinger equation $H|\Psi\rangle = E|\Psi\rangle$, the problem is reduced to the one-dimensional problem with parameters k_y and Φ as

$$-t_x\{\Psi_{m+1}(k_y,\Phi) + \Psi_{m-1}(k_y,\Phi)\} - 2t_y \cos\left(k_y - 2\pi\frac{\Phi}{L_y} - 2\pi\phi m\right) \Psi_m(k_y,\Phi) = E\Psi_m(k_y,\Phi). \qquad (2.3)$$

This is the Harper equation.[39,14,15] Equation (2.3) is represented in the following matrix form:

$$\begin{pmatrix} \Psi_{m+1}(\epsilon,k_y,\Phi) \\ \Psi_m(\epsilon,k_y,\Phi) \end{pmatrix} = \tilde{M}_m(\epsilon,k_y,\Phi) \begin{pmatrix} \Psi_m(\epsilon,k_y,\Phi) \\ \Psi_{m-1}(\epsilon,k_y,\Phi) \end{pmatrix}, \qquad (2.4)$$

$$\tilde{M}_m(\epsilon,k_y,\Phi) = \begin{pmatrix} -\epsilon - 2r\cos(k_y - 2\pi\frac{\Phi}{L_y} - 2\pi\phi m) & -1 \\ 1 & 0 \end{pmatrix}, \qquad (2.5)$$

where $\epsilon = \frac{E}{t_x}$ is a reduced energy and $r = \frac{t_y}{t_x}$ represents an anisotropy of the hoppings. (We do not explicitly write k_y and Φ dependence in the following.) We assume that the system size in the x direction is commensurate with the flux, that is, we assume $L_x = ql$ with some integer l. (We also discuss the incommensurate case later.) Then we get a reduced transfer matrix of the form

$$\begin{pmatrix} \Psi_{L_x+1}(\epsilon) \\ \Psi_{L_x}(\epsilon) \end{pmatrix} = [M(\epsilon)]^l \begin{pmatrix} \Psi_1 \\ \Psi_0 \end{pmatrix}, \qquad (2.6)$$

$$M(\epsilon) = \tilde{M}(\epsilon)_q \tilde{M}(\epsilon)_{q-1} \cdots \tilde{M}(\epsilon)_2 \tilde{M}(\epsilon)_1 = \begin{pmatrix} M_{11}(\epsilon) & M_{12}(\epsilon) \\ M_{21}(\epsilon) & M_{22}(\epsilon) \end{pmatrix}, \qquad (2.7)$$

where $M_{11}(\epsilon), M_{12}(\epsilon), M_{21}(\epsilon)$, and $M_{22}(\epsilon)$ are polynomials of ϵ with degree q, $q-1$, $q-1$, and $q-2$, respectively. All kinds of solutions are obtained by different choices of Ψ_0 and Ψ_1.

By this procedure, the problem of the two-dimensional electrons in a uniform magnetic field is reduced to the one-dimensional problem with parameter k_y and Φ. This is a problem of the discrete Hill equation[40] and there are several studies in the context of nonlinear lattice models.[41–44] Here we use and extend it to study the problem of the two-dimensional electrons under the magnetic field.[45]

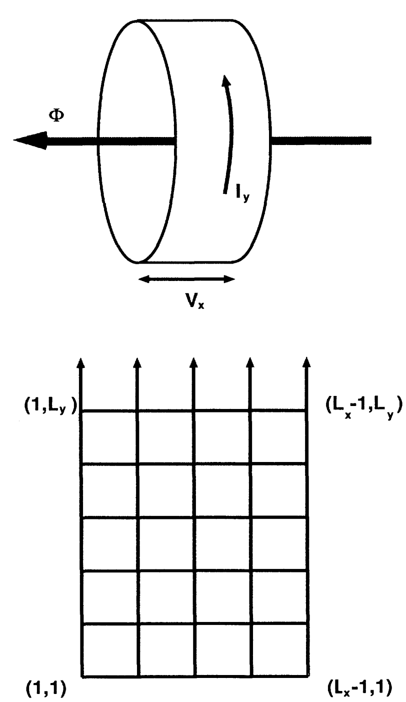

FIG. 1. The Laughlin-Halperin geometry which is used in our work. We assume that the system is on the square lattice. The system is periodic in the y direction and there are two edges $x = 1$ and $x = L_x - 1$.

III. ENERGY BANDS AND EDGE STATES

In this section, we investigate the spectrum of the one-dimensional problem given in the preceding section with special attention given to the edge states. The boundary condition of our problem is

$$\Psi_{L_x} = \Psi_0 = 0. \tag{3.1}$$

The eigenvalue problem Eq. (2.3) is replaced with an algebraic equation by choosing $\Psi_0 = 0$ and $\Psi_1 = 1$ for this boundary condition. The spectrum of the problem is discrete and given by the roots of the algebraic equation [see Eq. (2.6)]

$$\Psi_{L_x} = [M(\epsilon)^l]_{21} = 0. \tag{3.2}$$

From a direct calculation, we know that $[M(\epsilon)^l]_{21}$ is a polynomial of ϵ with degree $L_x - 1$ and has $L_x - 1$ real roots since they are eigenvalues of the Hermitian Hamiltonian.

First we point out that solutions of

$$M_{21}(\epsilon) = 0 \tag{3.3}$$

satisfy Eq. (3.2), since a product of tridiagonal matrices is also tridiagonal. We write the solutions of Eq. (3.3) as μ_j ($\mu_i < \mu_j$, $i < j$),[46] which are energies of edge states as we see just below.

In fact, Eq. (3.3) determines the energies of the edge states. From Eq. (2.6), we get

$$\Psi_{qk+1}(\mu_j) = [M_{11}(\mu_j)]^k \ . \tag{3.4}$$

If we use a usual normalized wave function[47] ($\sum_{m=1,L_x-1} |\Psi_m|^2 = 1$) and the number of sites $L_x - 1$ is sufficiently large, the state is exponentially localized at the edges as

$$|M_{11}(\mu_j)| < 1, \quad \text{localized at } x \approx 1 \text{ (left edge)} \tag{3.5}$$

$$|M_{11}(\mu_j)| > 1, \quad \text{localized at } x \approx L_x - 1 \text{ (right edge)} \ . \tag{3.6}$$

It proves that μ_j is the energy of the edge state. When $|M_{11}(\mu_j)| = 1$, the energy of the edge state degenerates with that of the extended bulk state at the band edge. In this case, the edge state is not localized exceptionally.

Equation (3.3) means that the wave function satisfies

$$\Psi_q = \Psi_0 = 0. \tag{3.7}$$

This is essentially a $g(=q - 1)$ sites problem with Eq. (2.3). The eigenvalues of the $g \times g$ matrix determines the energies of the edge states completely.

Here let us consider the problem in the periodic boundary condition for a while. There is an important relation between the spectrum of this fixed boundary system and that of the periodic system with an infinite size.[41,42,44] If we consider that the system is infinite in the x direction, our one-dimensional Hamiltonian Eq.(2.3) has a translational invariance with a period q. Then the Bloch (Floquet) theorem requires that the wave function of this infinite-size system satisfies

$$\Psi_{m+q}(\epsilon) = \rho(\epsilon)\Psi_m(\epsilon), \ |\rho(\epsilon)| = 1. \tag{3.8}$$

This should be compared with Eq. (3.7). We have to choose other set of Ψ_0 and Ψ_1 in this case. By applying this equation for $m = 0$ and 1, we know that ρ is an eigenvalue of M and ρ is a solution of

$$\rho^2 - \Delta(\epsilon)\rho + 1 = 0, \tag{3.9}$$

where

$$\Delta(\epsilon) = \mathrm{Tr} M = M_{11}(\epsilon) + M_{22}(\epsilon). \tag{3.10}$$

We used a fact

$$\det M(\epsilon) = M_{11}(\epsilon)M_{22}(\epsilon) - M_{12}(\epsilon)M_{21}(\epsilon) = 1, \tag{3.11}$$

since $\det \tilde{M}_m(\epsilon) = 1$ for all m.

There are several works about the spectrum of this periodic problem and we know that it consists of q energy bands[5,10,13–15,48,17] (continuous spectrum)

$$\epsilon \in [\lambda_1, \lambda_2], \ldots, [\lambda_{2j-1}, \lambda_{2j}], \ldots, [\lambda_{2q-1}, \lambda_{2q}], \quad (\lambda_i \le \lambda_j, \ i < j). \tag{3.12}$$

The energy bands are determined by the condition

$$[\Delta(\epsilon)]^2 \le 4. \tag{3.13}$$

On the other hand, the energies of the edge states μ_j satisfies $M_{11}M_{22} = 1$ by Eqs. (3.3) and (3.11). Then we have by Eq. (3.10)

$$[\Delta(\mu_j)]^2 = \left(M_{11} + \frac{1}{M_{11}}\right)^2 \ge 4. \tag{3.14}$$

It means μ_j lies in the energy gaps or at the band edges. Further we know that each gap has only one edge state[41,42,44]

$$\mu_j \in [\lambda_{2j}, \lambda_{2j+1}], \quad j = 1, \ldots, g(= q - 1), \tag{3.15}$$

where $[\lambda_{2j}, \lambda_{2j+1}]$ is the jth energy gap from below.

Here we have to notice that the boundary condition of our problem is not Eq. (3.7) but Eq. (3.1). Equation (3.1) has many solutions other than the solutions of Eq. (3.3). But we can show that these extra solutions are in the energy band regions. They are not the edge states but bulk states as shown in the following.

In the above, we consider the infinite-size system with period q. But it is also possible to consider that the period of the infinite system is $L_x(= lq)$. In this picture, the spectrum is composed of L_x bands as[49]

$$[\tilde{\lambda}_1, \tilde{\lambda}_2], \ldots, [\tilde{\lambda}_{2j-1}, \tilde{\lambda}_{2j}], \ldots, [\tilde{\lambda}_{2L_x-1}, \tilde{\lambda}_{2L_x}]. \tag{3.16}$$

However, the whole spectrum should remain unchanged. Thus the succeeding l bands should touch each other and compose one band as

$$\begin{aligned} \tilde{\lambda}_{2l(i-1)+2} &= \tilde{\lambda}_{2l(i-1)+3}, \\ &\ldots, \\ \tilde{\lambda}_{2l(i-1)+2j} &= \tilde{\lambda}_{2l(i-1)+2j+1}, \\ &\ldots, \\ \tilde{\lambda}_{2l(i-1)+2l-2} &= \tilde{\lambda}_{2l(i-1)+2l-1} \\ & i = 1, \ldots, q \ ; \ \ j = 1, \ldots, l-1. \end{aligned} \tag{3.17}$$

Using the same argument for Eq. (3.15), the energies of our boundary condition Eq. (3.1) are given by these degenerate energies $\tilde{\lambda}_{2l(i-1)+2j}$, $i = 1,\ldots,q$, $j = 1,\ldots,l-1$ (which are in the energy bands and those of the bulk states) and the energies of the edges states, μ_j, $j = 1,\ldots,g(= q-1)$. Counting the number of the roots, the above are all the solutions of our boundary condition Eq. (3.1) and all the edge states are given by μ_j, $j = 1,\ldots,g$.

When L_x is sufficiently large, the discrete spectrum of the fixed boundary condition should converge to the continuous energy bands and those of the edges states. Thus the spectrum is asymptotically given by the energy band Eq. (3.12) and isolated edges states μ_j in the $L_x \to \infty$ limit. In the following, we discuss the Hall conductance of the system with edges in the $L_x, L_y \to \infty$ limit. We should notice that even in this limit the spectrum is different from that of the usual infinite system due to the effect of the edge states.

IV. WINDING NUMBER OF THE EDGE STATE ON THE RIEMANN SURFACE

Let us consider the Bloch function at site q. The Bloch function is obtained by a different choice of Ψ_0 and Ψ_1 from those for the fixed boundary condition discussed above. For the Bloch function, Ψ_1 and Ψ_0 compose an eigenvector of M with the eigenvalue ρ [see Eqs. (2.4), (2.7) and (3.8)],

$$M(\epsilon)\begin{pmatrix}\Psi_1\\ \Psi_0\end{pmatrix} = \begin{pmatrix}\Psi_{q+1}(\epsilon)\\ \Psi_q(\epsilon)\end{pmatrix} = \rho(\epsilon)\begin{pmatrix}\Psi_1\\ \Psi_0\end{pmatrix}. \tag{4.1}$$

This equation is for real energy ϵ. In the following, let us extend the energy to a complex energy by an analytic continuation to discuss a wave function of the edge state. We use a complex variable z for the energy in this section.

We get from Eq. (4.1)

$$\rho(z) = \frac{1}{2}[\Delta(z) - \sqrt{\Delta(z)^2 - 4}], \tag{4.2}$$

and

$$\Psi_q(z) = -\frac{M_{11}(z) + M_{22}(z) - \sqrt{\Delta(z)^2-4}}{-M_{11}(z) + M_{22}(z) + \sqrt{\Delta(z)^2-4}} M_{21}(z), \tag{4.3}$$

where we used a normalization convention as $\Psi_1 = 1$. Since the analytic structure of the wave function is determined by the analytic function $\omega = \sqrt{\Delta(z)^2 - 4}$, let us discuss the Riemann surface of a hyperelliptic curve $\omega^2 = \Delta(z)^2 - 4$. To make the analytic structure of $\omega = \sqrt{\Delta(z)^2-4}$ unique, we have to specify the branch cuts of the function which are given by $\Delta(z)^2 - 4 \leq 0$ at $\Im z = 0$. Since this condition is the same as that of the energy bands Eq. (3.13), the branch cuts are given by the q energy bands. Thus $\Delta(z)^2 - 4$ is factorized by using energies of the band edges λ_j, $j = 1,\ldots,2q$ as

$$\begin{aligned}\omega &= \sqrt{\Delta(z)^2-4}\\ &= \sqrt{(z-\lambda_1)(z-\lambda_2)\cdots(z-\lambda_{2q-1})(z-\lambda_{2q})}.\end{aligned} \tag{4.4}$$

Also we have to use two sheets or Riemann spheres (R^+ and R^-) to define the Riemann surface (Fig. 2). (The Riemann spheres are obtained by compactifying the $|z| = \infty$ points to one point.)

Finally, the Riemann surface is obtained by gluing the two Riemann spheres at these q branch cuts along the arrows in the Fig. 2. After this gluing operation, the surface is topologically equivalent to the surface given in Fig. 3. The genus of the Riemann surface is $g = q - 1$, which is the number of the energy gaps. In this way, the wave function is defined on the genus g $(= q-1)$ Riemann surface (which is a complex energy surface).

The branch of the function is specified as

$$\sqrt{\Delta(z)^2-4} > 0 \quad (\ z \to -\infty \text{ on the real axis of } R^+). \tag{4.5}$$

Then if z lies in the jth gap from below on the real axis (notice that there are two real axes),

$$\alpha(-1)^j\sqrt{\Delta(z)^2-4} \geq 0,\ z \text{ (real) on } R^\alpha \ (\alpha = +,-). \tag{4.6}$$

At the energies of the edge states μ_j, $M_{11}M_{22} = 1$, and $\Delta^2 - 4 = (M_{11}+M_{22})^2 - 4 = (M_{11}-M_{22})^2$. By Eq. (4.6), it means

$$\sqrt{\Delta(\mu_j)^2-4} = \alpha(-1)^j|M_{11}(\mu_j) - M_{22}(\mu_j)| \qquad (\mu_j \in R^\alpha, \alpha = +,-). \tag{4.7}$$

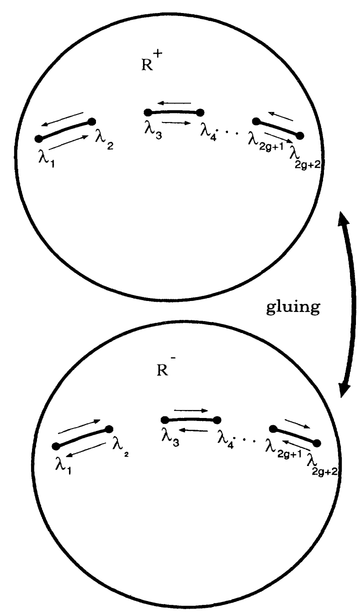

FIG. 2. Two sheets (Riemann spheres) with $q = g + 1$ cuts which correspond to the energy bands of the system. The Riemann surface of the Bloch function is obtained by gluing the two spheres along the arrows near the cuts.

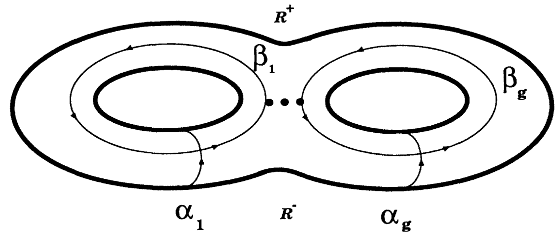

FIG. 3. Riemann surface of the Bloch function under the rational flux $\phi = p/q$. The number of the gaps g is the genus of the Riemann surface. α_j and β_j are the canonical loops (generators of the fundamental group) on the Riemann surface.

By Eqs. (4.3), (4.6), and (4.7), we get

$$\Psi_q(\mu_j + \delta) \approx -\frac{M_{11} + M_{22} - \alpha(-1)^j|M_{11} - M_{22}|}{-M_{11} + M_{22} + \alpha(-1)^j|M_{11} - M_{22}|} M_{21} \quad (\mu_j \in R^\alpha), \quad (4.8)$$

where $|\delta| \ll 1$.

By simple calculation, we can also show

$$\Delta(\epsilon) \leq -2 \text{ for } j \text{ odd}, \quad \geq 2 \text{ for } j \text{ even}, \quad (4.9)$$

where $\epsilon \in [\lambda_{2j}, \lambda_{2j+1}]$ (on $R^\pm$) when the energy ϵ is in the jth gap.

When $\Psi_q(\mu_j) = 0$ for $\mu_j \in R^\alpha$, $\Psi_q(\mu_j) \neq 0$ for $\mu_j \in R^{-\alpha}$ in general because $M_{21}(z)$ and the denominator of Eq. (4.8) vanish linearly at the point on this $R^{-\alpha}$ Riemann sheet.[46] In the following, we use a convention that μ_j denotes one of two $\mu_j \in R^\pm$ on the two Riemann sheets which gives the zero point of Ψ_q.

From Eqs (3.5), (3.6), (4.8), and (4.9), we get the following results.

The energy of the edge state μ_j gives a zero point of the Bloch function on the genus g ($\phi = p/q, g = q - 1$) Riemann surface. When the zero is on the upper sheet of the Riemann surface, the edge state is localized to the left, $x \approx 1$, edge. When the zero is on the lower sheet of the Riemann surface, the edge state is localized to the right, $x \approx L_x - 1$, edge.

The above considerations are all for the fixed k_y and Φ. As seen from Eq. (2.3), the spectrum is a function of $k_y - 2\pi\Phi/L_y$. Allowed values of k_y are discrete since our system is finite in the y direction. But we can change it almost continuously when L_y is sufficiently large. Even if L_y is small, we can extrapolate between different k_y by changing Φ. In the following, we consider k_y as a continuous variable for a while.

In Fig. 4 we show asymptotic energy spectrum of the two-dimensional tight-binding electrons with two edges under the rational flux $\phi = p/q$. The shaded areas are the asymptotic ($L_x \to \infty$) energy band regions and the lines are the spectrum of the edge states. The solid line means the edge state is localized at $x \approx 1$ and the dotted line means that it is localized at $x \approx L_x - 1$ [Eqs. (3.5) and (3.6)].

The Riemann surface of the Bloch function is given by the fixed k_y. In the following, let us consider a family of the Riemann surfaces parametrized by k_y. The surface is generally modified by changing k_y. However, the topology of the Riemann surface cannot be changed unless the energy gaps close. In other words, the topology of the Riemann surface does not change if there exist $g = q - 1$ energy gaps in the two-dimensional problem of the tight-binding electrons under the magnetic field *without boundaries*. We know that there is a degeneracy at the zero mode in the even q case.[16,10,48,17] Further, the gap closing phenomena occur when we include nearest-neighbor hoppings.[17] In these cases, the topology of the Riemann surface changes at some value of k_y and that brings an ambiguity of the quantized Hall conductance σ_{xy} since σ_{xy} is given by a topological number on this Riemann surface, as we show in the following. For example, we show the result for the $q = 6$ case in Fig. 4(d). It clearly shows the degeneracy at the zero energy.[48,10,17] The number of the degeneracies is 6, as expected. At these degenerate points, one of the holes of the Riemann surface collapses and the topology of the Riemann surface changes. We will comment on the effect of this topology change in relation to σ_{xy} later.

First of all, the spectrum is a periodic function of k_y with a period 2π. This means that the zero points of Ψ_q, that is, the energy of the edge state μ_j, form closed loops $C(\mu_j)$ on the Riemann surface by changing k_y from 0 to 2π. When μ_j moves to the different sheet of the Riemann surface, we get $M_{11}(\mu_j) = M_{22}(\mu_j) = \pm 1$, that is, μ_j has to be at the band edge. Using the above discussions, we can trace the movement of the μ_j on the Riemann surface in Fig. 4. The interesting fact is that this movement on the Riemann surface is not always monotonic [for example, see $C(\mu_3)$ in Figs. 4(a) and 4(b)].

On the genus g Riemann surface, the first homotopy group is generated by $2g$ generators, α_j and β_j, $j = 1, \ldots, g$ with the defining relation $\prod_{j=1}^g (\alpha_j \beta_j \alpha_j^{-1} \beta_j^{-1}) = \hat{1}$. See Fig. 3. The intersection number of these curves (including directions, Fig. 5) (Refs. 41 and 43) $I(\alpha_j, \beta_k)$ is given by

$$I(\alpha_j, \beta_k) = \delta_{jk}. \quad (4.10)$$

Any curves on the Riemann surface are spanned homotopically by α_j and β_j. We can observe that μ_j moves t times around the jth hole with some integer t, that is, homotopically

$$C(\mu_j) \cong \beta_j^t, \quad (4.11)$$

where t is an integer. This means that

$$I[\alpha_k, C(\mu_j)] = t\delta_{kj}, \quad (4.12)$$

even if the movement of μ_j is not monotonic. The intersection number is a standard mathematical object on the Riemann surface and a topological number.[43] It is essentially a winding number of the edge state around the jth hole.

Here we get the main results.

The winding number of the edge state μ_j, which is

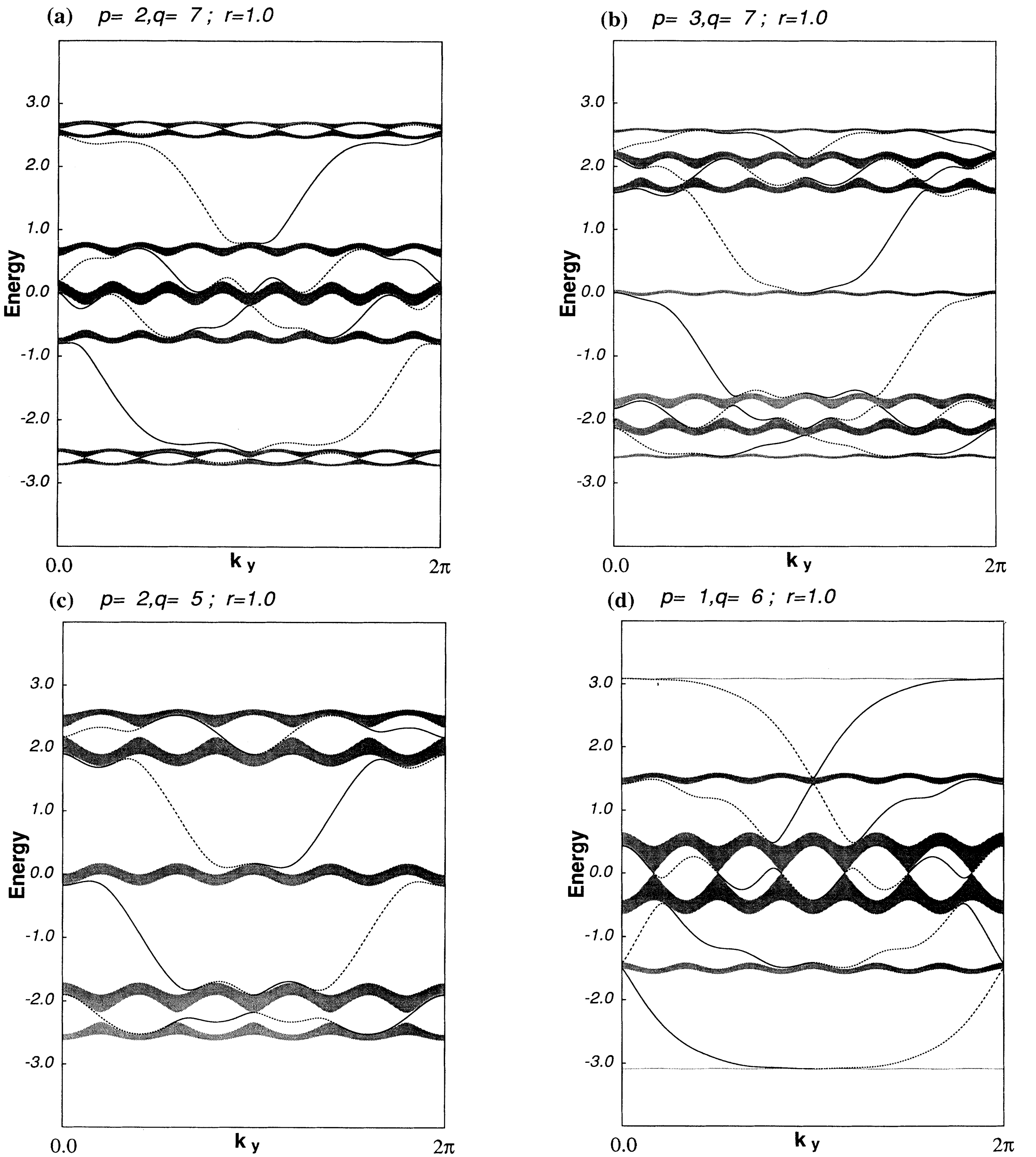

FIG. 4. Asymptotic energy spectrum of the two-dimensional tight-binding electrons with edges under the rational flux $\phi = p/q$. The number of sites in the x direction is $L_x - 1 \approx \infty$, but we assume that the size is commensurate with the flux ϕ as $L_x = ql$, where l is an integer. The shaded areas are the (asymptotically $L_x \to \infty$) energy bands and the lines are the spectrum of the edge states. The solid line means that the energy of the edge state is on the upper Riemann surface R^+ (the state is localized near $x \approx 1$) and the dotted line means that it is on the lower Riemann surface R^- (the state is localized near $x \approx L_x - 1$). (a) $\phi = 2/7$, $r = 1.0$ $C(\mu_1) \cong \beta_1^{-3}$, $C(\mu_2) \cong \beta_2^1$, $C(\mu_3) \cong \beta_3^{-2}$, $C(\mu_4) \cong \beta_4^2$, $C(\mu_5) \cong \beta_5^{-1}$, $C(\mu_6) \cong \beta_6^3$; (b) $\phi = 3/7$, $r = 1.0$, $C(\mu_1) \cong \beta_1^{-2}$, $C(\mu_2) \cong \beta_2^3$, $C(\mu_3) \cong \beta_3^1$, $C(\mu_4) \cong \beta_4^{-1}$, $C(\mu_5) \cong \beta_5^{-3}$, $C(\mu_6) \cong \beta_6^2$; (c) $\phi = 2/5$, $r = 1.0$, $C(\mu_1) \cong \beta_1^{-2}$, $C(\mu_2) \cong \beta_2^1$, $C(\mu_3) \cong \beta_3^{-1}$, $C(\mu_4) \cong \beta_4^2$; (d) $\phi = 1/6$, $r = 1.0$, $C(\mu_1) \cong \beta_1^1$, $C(\mu_2) \cong \beta_2^2$, $C(\mu_3) \cong \beta_3^x$, $x =$?, $C(\mu_4) \cong \beta_4^{-2}$, $C(\mu_5) \cong \beta_5^{-1}$. (At the third gap, the gap closes at some values of k_y. Then the topology of the Riemann surface changes and we cannot define the winding number without ambiguity.) (e) $\phi = 3/7$, $r = 0.5$; compare with (b).

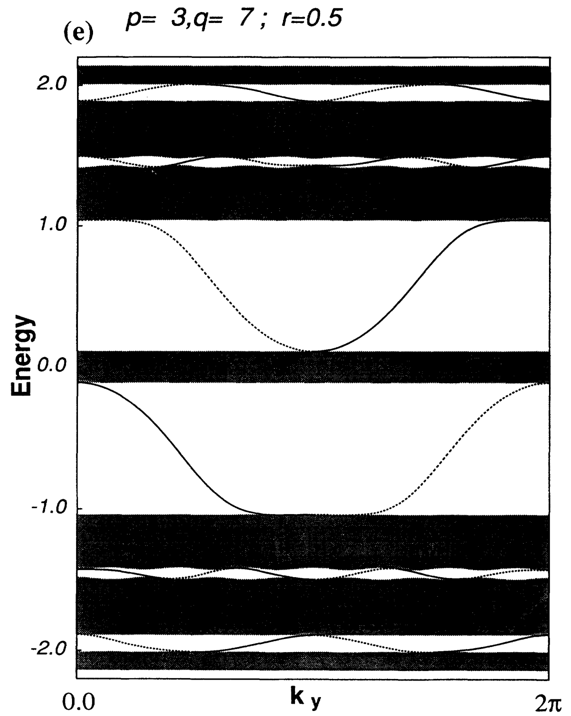

FIG. 4 *(Continued).*

given by the intersection number $I[\alpha_j, C(\mu_j)]$ between the canonical loop α_j on the Riemann surface and the trace of μ_j, $C(\mu_j)$, gives the quantized Hall conductance σ_{xy} when the Fermi energy lies in the jth gap

$$\sigma_{xy} = -\frac{e^2}{h} I[\alpha_j, C(\mu_j)]. \tag{4.13}$$

This means that the quantized Hall conductance is expressed by the topological number on the Riemann surface.

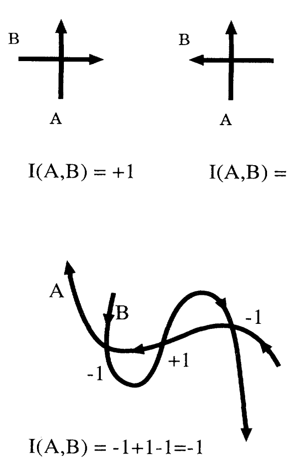

FIG. 5. Intersection number $I(A, B)$ of two curves A and B. Each intersection point contributes by $+1$ or -1 according to the direction.

This is understood from the following example using the Laughlin-Halperin argument.[2,4,50] Let us imagine that the Fermi energy lies in a gap such as Fig. 6. In the following, we consider the discreteness of the allowed k_y explicitly. In the ground state, some of the edge states are occupied, which are denoted by black circles and some of them are not occupied (white circles) (see the left-hand side of Fig. 6). Let us increase the central flux Φ from 0 to 1 adiabatically. All the states, including edges states and bulk states, are labeled by k_y. During the adiabatic process, the k_y state is shifted to the $k_y - 2\pi\Phi/L_y$ state. At the initial and final states, the spectrum is the same due to the gauge invariance. However, the state is not necessarily returned to the original state. In fact, the bulk states returned to the original states since the Fermi energy is in the energy gap. But the edge states do not return to the original state, as seen from the right-hand side of Fig. 6. The edge states carry currents in the process.

In this example, we know two states are carried from the right edge to the left edge, but one state is carried from the left to the right. In net, just one state is carried from the right to the left. (In this example, the winding number or the intersection number $I[\alpha_j, C(\mu_j)]$ is 1.) From this example, we are able to get a conclusion for general cases. In general, when the Fermi energy lies in the jth energy gap, $I[\alpha_j, C(\mu_j)]$ states are carried from the right edge ($x = L_x - 1$) to the left edge ($x = 1$) *in net* during the adiabatic process. The energy change of the process is $\Delta E = \{-I[\alpha_j, C(\mu_j)]\}(-e)V_x$, where V_x is a voltage in the x direction. By Byers and Yang's formula, the Hall current I_y is given by[51,2,4]

$$I_y = c\frac{\Delta E}{\Phi_0 \Delta\Phi} = \sigma_{yx} V_x = -\sigma_{xy} V_x, \tag{4.14}$$

where we write the flux quantum $\Phi_0 = hc/e$ explicitly.

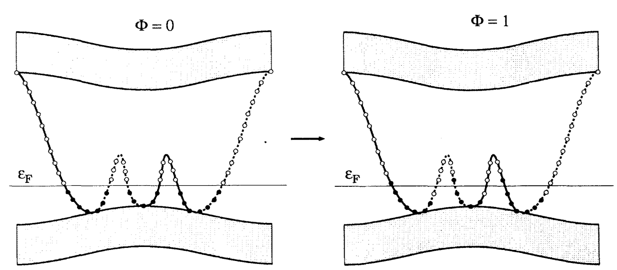

FIG. 6. Schematic figure of the edge states in the energy gap. (See Fig. 4.) Circles in the figure denote allowed k_y points of the edge states. In the left figure, the state is in the ground state. By changing the central flux by threading the hole of the system adiabatically from 0 to 1, the ground state is connected to the excited state as shown on the right-hand side of the figure. The solid line means that the state is localized on the left edge $x \approx 1$ and the dotted line means that it is localized on the right edge $x \approx L_x - 1$. We can count how many states are transported during the process by investigating the figure. This number is also related to the intersection number (winding number) of the curves (see text).

Then we get an expression for σ_{xy} as Eq. (4.13).

As shown by Kohmoto, the Hall conductance σ_{xy} is given by the first Chern number of the $U(1)$ fiber bundle on a torus (the magnetic Brillouin zone) (Ref. 8) and it is a topological invariant.[8,16] Mathematical treatments are also given by several authors.[30–32] Here we can relate σ_{xy} as a different topological number $I[\alpha_j, C(\mu_j)]$ on the Riemann surface of the Bloch function by investigating the edge states.

For an infinite system, we know that σ_{xy} is given by the solution of the following Diophantine equation for integers t and s:

$$j = sq + tp \equiv tp \ (\mathrm{mod}\ q), \quad |t| \leq q/2. \tag{4.15}$$

In this equation, we assume that the Fermi energy lies in the jth gap. The Hall conductance is quantized to $-t(e^2/h)$.[5,10,38] Here we get another method to calculate the σ_{xy} by calculating the winding number of the edge state. This means that $I[\alpha_j, C(\mu_j)]$ satisfies the Diophantine equation

$$j = sq + I[\alpha_j, C(\mu_j)]p \equiv I[\alpha_j, C(\mu_j)]p \ (\mathrm{mod}\ q). \tag{4.16}$$

(See Table I.)

We have performed extensive calculations for many cases ($q \lesssim 13$) and confirmed our integers obtained from counting the intersection number are the same as those given by the Diophantine equation. The Diophantine equation is originally derived in the anisotropic limit using perturbation theory.[5,10] For this anisotropic case, we also performed several numerical calculations. In Fig. 4(e) we show one example for the anisotropic case. Comparing it with the isotropic case (b), we know that the winding number is the same. Further, we know that the movement of the zero point on the Riemann surface is monotonic. It seems possible to derive the Diophantine equation directly from our treatment for the Hall conductance. Here, we give a rough argument about this fact in the Appendix.

Here we comment on the degeneracies of the energy bands which occur in some situations.[10,48,17] One of the examples is at the third gap in the $\phi = 1/6$ case [see Fig 4(d)]. Except for the third gap, we can define the winding numbers safely. For the third gap, however, one of the g (=5) holes of the Riemann surface collapses at these degenerate points. At the points, the topology of the Riemann surface changes and the winding number is not well defined. It corresponds to the ambiguity of σ_{xy}. At the degenerate points, two energy bands degenerate and, further, the energy of the edge state also degenerate.[52] If we include next-nearest-neighbor hoppings, this degeneracies are removed and we will get a well-defined winding number for this case.[22,17,53] In general, the Hall conductance can only be changed by this topological change of the Riemann surface.

TABLE I. Solutions of the Diophantine equation corresponding to Fig. 4. Compare with the winding numbers in Fig. 4.

	$j = sq + tp$		
$\phi = p/q$	jth gap	$t : \sigma_{xy} = (e^2/h)\ t$	s
$\phi = 2/7$	1	-3	1
	2	1	0
	3	-2	1
	4	2	0
	5	-1	1
	6	3	0
$\phi = 3/7$	1	-2	1
	2	3	-1
	3	1	0
	4	-1	1
	5	-3	2
	6	2	0
$\phi = 2/5$	1	-2	1
	2	1	0
	3	-1	1
	4	2	0
$\phi = 1/6$	1	1	0
	2	2	0
	3	?	?
	4	-2	1
	4	-1	1

V. INCOMMENSURATE CASE AND RANDOM POTENTIAL

In Sec. IV we considered the commensurate case $L_x = ql$. In this section, first we treat incommensurate cases and discuss effects of the randomness later.

For the incommensurate case, we do not have good methods to obtain the asymptotic spectrum. We have to solve the one-dimensional Schrödinger equation Eq. (2.3), under the boundary condition $\Psi_0 = \Psi_{L_x} = 0$. In Fig. 7, we show results for the case $p = 2, q = 7$, and $L_x = 126$. Let us compare Fig. 7 with Fig. 4(a), which corresponds to the commensurate case. The system size is not so large in Fig. 7, but the energies in the energy band regions seem to converge to the same one. It suggests that the bulk states do not depend on the commensurability. On the other hand, the behavior of the edge states in Fig. 7 differs from that of the Fig. 4(a). We cannot identify the energy of the edges states as that of the zero point of the Bloch function in this incommensurate case. However, there still exists a similarity between these two results. If we shift the energies of the edge states as a function of k_y, it seems that we can get the same shape of the spectrum as that of the commensurate case. For the Hall conductance σ_{xy}, we can get the same results as that of the commensurate case by investigating the wave functions of the edge states numerically (investigating which side the edge state localizes). We can confirm that the number of the carried states during the adiabatic process (discussed at the end of Sec. IV) is the same as that of the commensurate case. This means that the edges states are sensitive to the commensurability, but the Hall conductance is the same as that of the commensurate case.

Next we discuss the effect of the randomness. As is well known, the existence of the randomness is necessary to

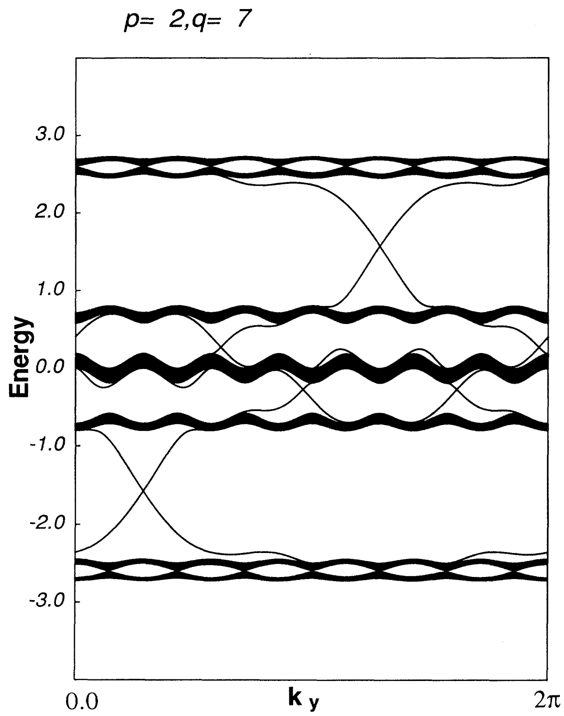

FIG. 7. Energy spectrum of the two-dimensional tight-binding electrons with two edges under the rational flux $\phi = p/q$. The system size in the x direction is incommensurate with the flux q. $p = 2$, $q = 7$, $L_x = 127$, and $t_x = t_y = 1$. Compare with Fig. 4(a).

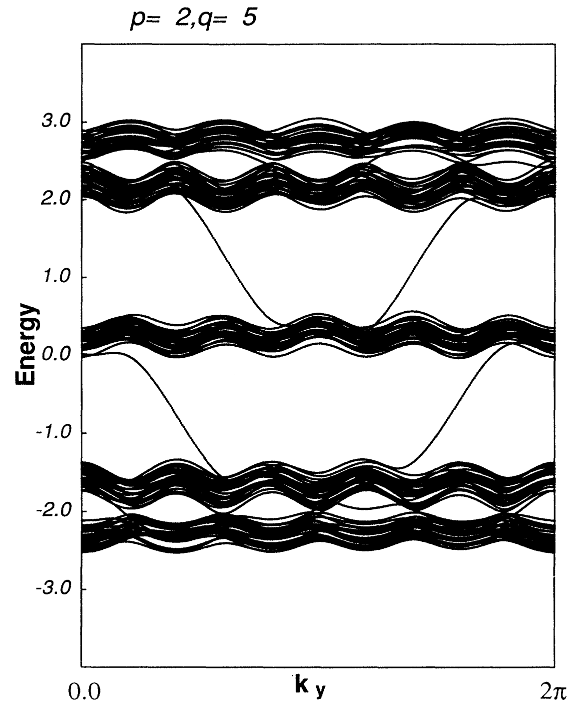

FIG. 8. Energy spectrum of the two-dimensional tight-binding electrons with two edges under the rational flux $\phi = p/q$ where we include an effect of a one-"dimensional" random potential $t_x = t_y = 1$, $V_{rnd} = 0.5$, $p = 2, q = 5$, and $L_x = 125$ for the commensurate case. See the text, and compare with Fig. 4(c).

explain the quantum Hall effect.[2–4,11] however, it is very difficult to completely include effects of the randomness in the large system.[54] Here we introduce rather artificial *one-dimensional randomness* in the two-dimensional system. The Hamiltonian is given by

$$H + \sum_{n,m} V(m) c^{\dagger}_{m,n} c_{m,n}, \tag{5.1}$$

where we assume $V(m)$ is a uniform random number between $[-V_{rnd}, V_{rnd}]$ and H is defined in Eq. (2.1). This potential is random in the x direction, but uniform in the y direction. We consider that bulk properties such as the localization are really crucial to the dimensionality. However, as far as the edges state is concerned, we hope that the artificial one-dimensional randomness still includes some effects of the true two-dimensional randomness. We can perform a Fourier transformation in the y direction and the spectrum of the system is obtained almost similarly to the previous incommensurate case.

We show the spectrum of the system for $p = 2, q = 5$, and $L_x = 125$ with randomness $V_{rnd} = 0.5t_x$ in Fig. 8. Let us compare Fig. 8 with Fig. 4(c). It seems that there still exist edge states in this random system. For the second and third gaps, we can clearly distinguish the edge states from the bulk states. When the Fermi energy lies in these gaps, we can do the same argument as that of Sec. IV and obtain the quantized value of the Hall conductance.

In the first or fourth energy gaps, however, there are several level crossings. Thus we cannot perform the adiabatic process discussed in Sec. IV. This means that σ_{xy} is not well quantized when the Fermi energy is in these energy gaps. By this argument, we believe the quantization is more accurate when the Fermi energy lies in the larger energy gap.

The point of the above argument is that we have to treat one (macroscopic) Schrödinger equation even if there is a randomness in the system. We consider that usual averaging procedures to treat the randomness are not suitable to discuss the quantized Hall conductance especially for the edge states.

VI. SUMMARY

In this paper, we consider the edge states of the two-dimensional electron systems on a square lattice under a rational magnetic field $\phi = p/q$. The system is periodic in the y direction and there are two edges in the x direction. This is the Laughlin-Halperin geometry. Due to this geometry, there are several edge states. We have studied the behavior of edge states carefully. Performing a Fourier transformation in the y direction, we can reduce this problem to the problem in one dimension.

We found that the zero points of the Bloch function give the energies of the edge states. The Bloch function is defined on the Riemann surface (complex energy surface) with the genius $g = q-1$, which is the number of the gaps as a two-dimensional problem. The energy of the edge state moves around the hole of the Riemann surface when we change the momentum in the y direction. When the Fermi energy lies in the jth gap, the winding number of the edge state around the jth hole (energy gap) gives the Hall conductance of the system. The winding number is given by the intersection number of two curves on the Riemann surface. One is the trace of the energy of the edge state and the other is a canonical curve on the Riemann surface. It is a topological number on the Riemann surface. In this sense, we can express the Hall conductance as a new kind of the topological number. The effects of the randomness is also investigated using a kind of artificial one-dimensional random potential. The stability of the quantization of the Hall conductance is also mentioned. Since the edge states are stable to the weak disorder, we expect that the present topological consideration of the Hall conductance is relevant in the realistic system.

ACKNOWLEDGMENTS

The author thanks A. Zee, M. Kohmoto, B. I. Halperin, Y. S. Wu, T. Ando, X. G. Wen, and P. A. Lee for helpful discussions about the edge states. He especially thanks A. Zee and M. Kohmoto for careful reading of the manuscript and useful comments. He thanks M. Kohmoto for discussions about the TKNN work and the related topics. He also thanks K. Iguchi for informing him about Ref. 41. He is grateful to the Institute for Theoretical Physics (Santa Barbara) for hospitality. The work was supported in part by the National Science Foundation under Grant No. PHY89-04035. It was also supported in part by a Grant-in-Aid for Scientific Researches on Priority Areas "Computational Physics as a New Frontier in Condensed Matter Research" and on the Promotion for the Young Scientists from the Ministry of Education, Science and Culture, Japan.

APPENDIX: DIOPHANTINE EQUATION

In this appendix, we show rough arguments for the Diophantine equation by investigating the edge states. Using a perturbation theory, we will argue that the intersection numbers discussed in this work coincide with the solutions of the Diophantine equation in the absolute values. To determine the sign, we have to investigate the wave function more carefully.

Let us consider an anisotropic limit $r = t_y/t_x \ll 1$. As discussed in Sec. III, the energies of the edge states are determined by the $g \times g$ matrix since it is essentially a $g = q - 1$ site problem [see Eq. (3.7)]. The $g \times g$ matrix, which determines energies of the edge states, is

$$\mathbf{H}_e = \mathbf{H}_0 + \mathbf{H}_1, \tag{A1}$$

where

$$(\mathbf{H}_0)_{ij} = -(\delta_{i,j+1} + \delta_{i+1,j}), \tag{A2}$$

$$(\mathbf{H}_1)_{ij} = -2r\delta_{ij}\cos(k_y - 2\pi\phi j). \tag{A3}$$

The energy of the jth edge state, μ_j, is the jth eigenvalue of the $\mathbf{H}_e$. In zeroth order in r, the energies of the edge states μ_j are given by

$$\mu_j^{(0)} = -2\cos\left(\frac{\pi}{q}j\right), \tag{A4}$$

where a normalized vector corresponding to the jth energy $\mathbf{U}_j$ is given by

$$(\mathbf{U}_j)_k = \sqrt{\frac{2}{q}}\sin\left(\frac{\pi}{q}jk\right). \tag{A5}$$

Using this vector it is easy to calculate a first-order correction to the energy of the edge state. It is given by

$$\begin{aligned}\mu_j^{(1)} &= (\mathbf{U}_j, \mathbf{H}_1\mathbf{U}_j)\\ &= (-2r)\sum_{k=0}^{g}\frac{2}{q}\sin^2\left(\frac{\pi}{q}jk\right)\cos\left(k_y - 2\pi\frac{p}{q}k\right)\\ &= \frac{2r}{q}\sum_{k=0}^{g}\left\{\cos\left[\frac{2\pi}{q}(j-p)k + k_y\right]\right.\\ &\qquad\left. + \cos\left[\frac{2\pi}{q}(j+p)k - k_y\right]\right\}\\ &= 2r\cos(k_y)[\delta(j-p\equiv 0) + \delta(j+p\equiv 0)],\end{aligned} \tag{A6}$$

where $\equiv$ is in [mod q]. It means that the first-order perturbation contributes only to two cases,

$$j = j_\pm = \pm p + sq, \tag{A7}$$

with some integer s ($1 \le j_\pm \le g$). Then the energies of edge states are given up to the first order by

$$\mu_j \approx \begin{cases} -2\cos\left(\frac{\pi}{q}j\right) + 2r\cos(k_y), & j = j_\pm \\ -2\cos\left(\frac{\pi}{q}j\right) & \text{otherwise.}\end{cases} \tag{A8}$$

This means that the winding number (or) the intersection number $I[\alpha_{j_\pm}, C(\mu_{j_\pm})]$ is $+1$ or -1 if the movement of $\mu_{j_\pm}$ is monotonic on the Riemann surface [see Fig. 4(e)]. To determine its sign (direction of the winding), more detailed investigation is necessary. For $j \ne j_\pm$, we have to consider a higher perturbation.

We assume that the perturbation Hamiltonian first contributes the energy $\mu_{j_{\pm t}}$ in the tth order. Then we estimate the contributes to the energies very roughly by

$$\mu_{j_{\pm t}}^{(t)} \approx \frac{\text{const}}{(\Delta\epsilon_{j_{\pm t}})^{t-1}}(\mathbf{U}_{j_{\pm t}}, \mathbf{H}_1^t\mathbf{U}_{j_{\pm t}}), \tag{A9}$$

$$\mu_{j_{\pm t}}^{(i)} = 0 \quad (i < t), \tag{A10}$$

where $\Delta\epsilon_{j_{\pm t}}$ is a contribution from an energy denominator.

Then we know that the following terms contribute to the energies $\mu_{j_{\pm t}}$ *first* in tth order:

$$\mu^{(t)}_{j_{\pm t}} \approx \text{const}\, r^t \sum_{k=0}^{g} \left[\cdots + \cos\left\{ \frac{2\pi}{q}(j_{\pm t} - tp)k + tk_y \right\} + \cos\left\{ \frac{2\pi}{q}(j_{\pm t} + tp)k - tk_y \right\} \right],$$
$$\approx \text{const}\, r^t \cos(tk_y)[\delta(j_{\pm t} - tp \equiv 0) + \delta(j_{\pm t} + tp \equiv 0)] + \cdots, \quad \text{(A11)}$$

where $(\cdots)$ does not contribute to to the $\mu_{j_{\pm t}}$. Here $j_{\pm t}$ is defined by

$$j_{\pm t} = \pm tp + sq, \quad \text{(A12)}$$

with some integer s $(1 \le j_{\pm t} \le g)$. Then up to tth order

$$\mu_{j_{\pm t}} \approx -2\cos\left(\frac{\pi}{q} j_{\pm t}\right) + \text{const}\, r^t \cos(tk_y). \quad \text{(A13)}$$

Equation (A13) shows that the intersection number $I[\alpha_{j_{\pm t}}, C(\mu_{j_{\pm t}})]$ is $+t$ or $-t$ if the movement of $\mu_{j_{\pm t}}$ is monotonic on the Riemann surface. [See Fig. 4(e).]

---

*Permanent address: Institute for Solid State Physics, University of Tokyo, 7-22-1 Roppongi, Minato-ku, Tokyo 106, Japan; electronic address: hatsugai@tansei.cc.u-tokyo.ac.jp

[1] K. V. Klitzing, G. Dorda, and M. Pepper, Phys. Rev. Lett. **45**, 494 (1980).
[2] R. B. Laughlin, Phys. Rev. B **23**, 5632 (1981).
[3] H. Aoki and T. Ando, Solid State Commun. **38**, 1079 (1981).
[4] B. I. Halperin, Phys. Rev. B **25**, 2185 (1982).
[5] D. J. Thouless, M. Kohmoto, P. Nightingale, and M. den Nijs, Phys. Rev. Lett. **49**, 405 (1982).
[6] A. Widom, Phys. Lett. **90A**, 474 (1982).
[7] P. Strěda, J. Phys. C **15**, L717 (1982).
[8] M. Kohmoto, Ann. Phys. (N. Y.) **160**, 355 (1985).
[9] Q. Niu, D. J. Thouless, and Y. S. Wu, Phys. Rev. B **31**, 3372 (1985).
[10] M. Kohmoto, Phys. Rev. B **39**, 11 943 (1989).
[11] *The Quantum Hall Effect*, edited by R. E. Prange and S. M. Girvin (Springer-Verlag, Berlin, 1987).
[12] J. Zak, Phys. Rev. **134**, A1602 (1964); *ibid.* **134**, 1607 (1964).
[13] M. Ya. Azbel, Zh. Eksp. Teor. Fiz. **46**, 929 (1964) [Sov. Phys.—JETP **19**, 634 (1964)].
[14] D. R. Hosfstadter, Phys. Rev. B **14**, 2239 (1976).
[15] G. H. Wannier, Phys. Status Solidi B **88**, 757 (1978); G. H. Wannier, G. M. Obemaier, and R. Ray, *ibid.* **93**, 337 (1979).
[16] J. Avron, R. Seiler, and B. Simon, Phys. Rev. Lett. **51**, 51 (1983).
[17] Y. Hatsugai and M. Kohmoto, Phys. Rev. B **42**, 8282 (1990).
[18] I. Affleck and J. Marston, Phys. Rev. B **37**, 3774 (1988); G. Kotliar, *ibid.* **37**, 3663 (1988).
[19] Y. Hasegawa, P. Lederer, T. M. Rice, and P. B. Wiegmann, Phys. Rev. Lett. **63**, 907 (1989).
[20] M. Kohmoto and Y. Hatsugai, Phys. Rev. B **41**, 9527 (1990).
[21] Y. Hasegawa, Y. Hatsugai, M. Kohmoto, and G. Montambaux, Phys. Rev. B **41**, 9174 (1990).
[22] X. G. Wen, F. Wilczek, and A. Zee, Phys. Rev. B **39**, 11 413 (1989).
[23] H. Fukuyama, O. Narikiyo, and K. Kuboki, J. Phys. Soc. Jpn. **59**, 807 (1990).
[24] A. Zee, Int. J. Mod. Phys. B **5** 529 (1991); A. Zee, *Proceedings of the Brazilian Winter School* (World Scientific, Singapore, in press).
[25] Y. Hasegawa (unpublished).
[26] B. I. Halperin, J. Appl. Phys. Suppl. **26**, 1913 (1987).
[27] G. Montambaux and M. Kohmoto, Phys. Rev. B **41**, 11 417 (1990).
[28] M. Kohmoto, B. I. Halperin, and Y. S. Wu, Phys. Rev. B **45**, 13 488 (1992).
[29] Z. Kunszt and A. Zee, Phys. Rev. B **44**, 6842 (1991).
[30] A. Connes, Publ. Math. IHES **62**, 257 (1986).
[31] J. Bellisard, *Statistical Mechanics and Field Theory: Mathematical Aspect* (Springer-Verlag, Berlin, 1986).
[32] J. Avron and R. Seiler. Phys. Rev. Lett. **54**, 259 (1985).
[33] R. Rammal, G. Toulouse, M. T. Jaekel, and B. I. Halperin, Phys. Rev. B **27**, 5142 (1983).
[34] L. Schweizer, B. Kramer, and A. MacKinnon, J. Phys. C **17**, 4111 (1984); R. Johnstn, B. Kramer, and A. MacKinon, Surf. Sci. **170**, 256 (1986).
[35] A. H. MacDonald, Phys. Rev. B **29**, 6563 (1984).
[36] A. H. MacDonald and P. Streda, Phys. Rev. B **29**, 1616 (1984).
[37] S. N. Sun and J. P. Ralston, Phys. Rev. B **44**, 13 603 (1991).
[38] I. Dana, Y. Avron, and J. Zak, J. Phys. C **18**, L679 (1985).
[39] P. G. Harper, Proc. Phys. Soc. London Sect. A **68**, 874 (1955).
[40] The Harper equation is the simplest case of the discrete Hill equation.
[41] M. Toda, *Theory of Nonlinear Lattices* (Springer-Verlag, Berlin, 1981), and references therein.
[42] E. Date and S. Tanaka, Prog. Theor. Phys. **55**, 457 (1976); Prog. Theor. Phys. **59**, 107 (1976).
[43] D. Mumford, *Tata Lectures on Theta I, II* (Birkhäuser, Boston, 1983).
[44] H. P. McKean and P. von Moerbeke, Invent. Math. **30**, 217 (1974); H. P. McKean and E. Trubowitz, Commun. Pure. Appl. Math. **29**, 143 (1976).
[45] The theory of the nonlinear lattice is applied to a problem of the quasicrystal by K. Iguchi, J. Math. Phys. (to be published).
[46] All roots of $M_{21}(\epsilon)$ are simple (see Refs. 41 and 42).
[47] $\Psi_{qk+k'}$, $k' = 1, \ldots, q$ are also in the same order as Ψ_{qk+1} in general.
[48] X. G. Wen and A. Zee, Nucl. Phys. B **316**, 641 (1989).
[49] These energies $\tilde{\lambda}_j$ are determined by $[\text{Tr}\ M(\tilde{\lambda}_j)^l]^2 = 4$, similar to Eq. (3.13).
[50] Charge transport is also discussed in the following references. Z. Tešanović, F. Axel, and B. I. Halperin, Phys. Rev. B **39**, 8525 (1989); H. Kunz, Phys. Rev. Lett. **57**, 1095 (1986); D. J. Thouless, Phys. Rev. B **27**, 6083 (1983); A. H. MacDonald, *ibid.* **28**, 6713 (1983).
[51] N. Byers and C. N. Yang, Phys. Rev. Lett. **7**, 46 (1961).

[52]These degenerate zero modes in the infinite system were investigated using the topological method of Wen and Zee (Ref. 48) in detail.

[53]Even if we include the next-nearest-neighbor hoppings, it is still possible to reduce the problem to that of the one-dimensional one (Ref. 17) and to define the Riemann surface of the Bloch function.

[54]Effects of the randomness on a lattice in a finite-size cylinder geometry is discussed numerically by H. Aoki, J. Phys. C **18**, L67 (1985).